Formation of a two-kink soliton pair in perturbed sine-Gordon models due to kink–internal-mode instabilities

Mónica A. García-Ñustes* and Jorge A. González
Centro de Física, Instituto Venezolano de Investigaciones Científicas, Apartado 21827, Caracas 1020-A, Venezuela
(Received 11 November 2011; revised manuscript received 30 October 2012; published 14 December 2012)

The existence of two-kink soliton solutions in polynomial potentials was first reported by Bazeia *et al.* in a special type of scalar field systems [Phys. Rev. Lett. **91**, 241601 (2003)]. A general feature of these potentials is that they possess two minima and a local metastable minimum between them. In the present work we investigate the appearance of this special kind of soliton in the sine-Gordon model under the perturbation of a space-dependent force. We show that a pair of solitons is emitted during the process of kink breakup by internal mode instabilities. A possible explanation of these phenomena is an interplay between the solitons repelling interaction and the external force, resulting in a separation or a packing of several kinks.

DOI: 10.1103/PhysRevE.86.066602 PACS number(s): 05.45.Yv, 11.10.Lm, 98.80.Cq

I. INTRODUCTION

The appearance of kink solitons in scalar field models such as ϕ^4 and sine-Gordon (SG) models depends on the configuration of the energy potential $U(\phi)$. When the potential has, at least, two minima, the system exhibits a solution that connects both energetic states [1]. For example, in the case of a ϕ^4 model the solution connects the potential minima $\overline{\phi} = \pm 1$. In the SG case, the potential supports infinite minima. Thus, if ϕ varies only from 0 to 2π, the kink soliton interpolates between the two adjacent minima $\overline{\phi} = 0, 2\pi$. In general, it has been proved that depending on the shape of the potential $U(\phi)$ various classes of localized solutions in the form of kinks, pulses, and semisolitons are possible [2].

An interesting variation of kink soliton is the two-kink soliton introduced by Bazeia *et al.* [3,4] These solutions are present in a family of models described by polynomial potentials $U_p(\phi)$ in (1,1) dimensions which support minima at $\phi = 0$ and ± 1 for odd values of the control parameter p. The solution connects the minima $\phi = \pm 1$ passing through the local minimum at $\phi = 0$. Therefore, the two-kink soliton profile consists of two standard kinks separated by a distance which is proportional to p, the parameter that specifies the potential.

However, further investigations [5,6] revealed that the two-kink solution can be observed in models whose potentials are controlled by a parameter and not by the degree of the self-interacting scalar field. In other words, the energy configuration of the potential can be changed by a control parameter.

The two-kink soliton has received attention by its implications in the field of string theory and specially in the brane world [5–7]. Notwithstanding, experimental realization of such systems are rather complicated. A more usual physical scenario for studies in kink dynamics has been found in the long Josephson junction (LJJ) and its discrete version called the Josephson array. A regular kink in LJJs corresponds to a Josephson vortex or fluxon, a quantum of magnetic flux, which is well described by the SG kink solution. The fusion of two regular fluxons (kinks) into a bound state (two-kink state) has been already reported in an annular Josephson array subject to a constant bias current [8–10]. Similar solutions called multikinks have been reported in the discrete version of the SG model, also known as the Frenkel-Kontorova model with higher order dispersive terms [11,12]. These suggests that the two-kink solution can be observed and controlled in a more physically realizable scenario.

In the present work, we analyze the necessary conditions under which the formation of a two-kink soliton is possible in a perturbed SG model, following the general approach introduced in Ref. [13]. This procedure allows us to conduct an exact stability analysis of the internal modes when the system is perturbed by a suitable space-dependent force.

This work is organized as follows. In Sec. II, we review the exact stability analysis approach in the SG model perturbed by a external force. We report the observation of the two-kink soliton produced by a kink breakup. In Sec. III we show the main numerical results performed using a perturbed SG model. An expression of the energy that permits us to predict and control the two-kink formation is derived in Sec. IV. An analysis of the required conditions for the appearance of the two-kink and even the multikink (antikink) is given in Sec. V. In Sec. VI we present a possible experimental setup based on Josehpson junctions to study the formation of multikinks via internal mode instabilities. Finally we present our concluding remarks in Sec. VII.

II. STABILITY ANALYSIS

The sine-Gordon model has been applied in many branches of physics as particle physics and condensed matter theory. The model can describe many phenomena from domain walls in ferromagnets and fluxons in long Josephson junctions in solid state physics [14,15] to DNA models in biology [16].

In the unperturbed version of the SG model, the solution does not have internal modes. However, following the stability analysis technique, it has been shown that when the system is perturbed by an inhomogeneous external force, SG soliton internal modes can exist. Furthermore, inhomogeneous perturbations of the soliton equations in the form of both

*Current address: Departamento de Física, Facultad de Ciencias Físicas y Matemáticas, Universidad de Chile, Casilla 487-3, Santiago, Chile; mgarcianustes@ing.uchile.cl

external forces or parametric impurities generate effective potentials for the motion of the kink; i.e., the zeros of $F(x)$ represent equilibrium positions for the kink (antikink). The activation of extra internal modes and the zeros of the force can lead to the appearance of different phenomena such as kink explosion, tunneling escape from potential wells, and creation of a kink-antikink pair, among others [13,17–19].

To understand the conditions for the appearance of a two-kink soliton solution, we review the stability conditions for a kink in the presence of an inhomogenous external force $F(x)$, with at least one x_* such that $F(x_*) = 0$ [13].

The perturbed Klein-Gordon equation is

$$\phi_{tt} - \phi_{xx} + \frac{\partial U}{\partial \phi} = F(x), \tag{1}$$

where $U(\phi)$ is a potential that possesses at least two minima. The sine-Gordon and ϕ^4 equations are particular examples of (1) when $F(x) = 0$.

To solve exactly the stability problem, it is necessary to build a general function ϕ_k with the topological properties of the kink-soliton solution. Then, via an inverse problem, we are able to obtain a suitable $F(x)$ with the properties of the physical system under study. In particular, if $F(x)$ possesses only one zero ($F(x_*) = 0$) and $\frac{\partial F(x)}{\partial x}|_{x=x_*} > 0$, then the point $x = x_*$ is a stable (unstable) equilibrium position for the kink (antikink). Otherwise, if $\frac{\partial F(x)}{\partial x}|_{x=x_*} < 0$, the equilibrium position $x = x_*$ is unstable (stable) for the kink (antikink).

Considering $\phi(x,t) = \phi_k(x) + f(x)e^{\lambda t}$ and performing a linear stability analysis we get the following eigenvalue problem:

$$\hat{L} f = \Gamma f, \tag{2}$$

where $\hat{L} = -\partial_x^2 + \{\frac{\partial^2 U}{\partial u^2}|_{\phi=\phi_k(x)}\}$ and $\Gamma = -\lambda^2$. The translational and internal shape modes associated to the kink can be obtained from (2). For further explanations read [13,17–19] and references therein.

Let us look at the perturbed SG model

$$\phi_{tt} - \phi_{xx} + \sin\phi = F(x), \tag{3}$$

where

$$F(x) = \frac{2(B^2-1)\sinh(Bx)}{\cosh^2(Bx)} \tag{4}$$

is an external force with a single zero (or equilibrium position for the kink soliton) in $x_* = 0$.

The exact stationary solution of Eq. (3) is $\phi_k(x) = 4\arctan[\exp(Bx)]$. This solution represents a kink-soliton at the position $x = 0$. The stability problem (2) can be solved exactly. The eigenvalues of the discrete spectrum are given by the formula

$$\Gamma_n = B^2(\Lambda + 2\Lambda n - n^2) - 1, \tag{5}$$

where $\Lambda(\Lambda+1) = \frac{2}{B^2}$.

The integer part of Λ ($[\Lambda]$) yields the number of eigenvalues in the discrete spectrum, which correspond to the soliton modes (including the translational mode Γ_0, and the internal shape modes $\Gamma_n (0 < n < [\Lambda])$. Everything concerning the stability of the soliton in this situation can be obtained from the equation for Γ_n.

The parameter B acts as a control parameter. For $B^2 > 1$, the translational mode is stable, and there are no internal (shape) modes. In this regime the kink stays at the equilibrium position ($x_* = 0$). If $1/3 < B^2 < 1$, then the translational mode is unstable, but there are no internal modes. The kink moves from its unstable equilibrium position without shape deformations. When $1/6 < B^2 < 1/3$, the translational mode and one internal shape mode arise. This internal shape mode is stable. For $B^2 < 1/6$ many other internal modes can appear. For $B^2 < 2/[\Lambda_*(\Lambda_*+1)]$, where $\Lambda_* = (5+\sqrt{17})/2$, the first internal mode becomes unstable. This instability leads to a kink breakup by an internal shape instability [13,17,19].

The study of internal modes can give an insight of the underneath kink dynamics. Different phenomena as length-scale competition can be understood based on stability conditions [20]. Despite the particular construction of the external force, any physical model topologically equivalent will exhibit the same dynamical behavior around an equilibrium position. This scenario is also valid for any $F(x)$ with several zeros. Additionally, the stability conditions are stated in terms of the control parameter B. Therefore, we can easily control the kink dynamics by varying the external force parameters. This is specially important in experimental realizations of these physical systems.

Previous numerical simulations performed close to the threshold $B^2 < 2/[\Lambda_*(\Lambda_*+1)]$ have shown the emission of a kink-antikink pair. However, for lower values of B, below the threshold, there is not any numerical exploration. Indeed, our main focus is to explore numerically this region. In the next section, we show our main numerical results in this direction.

III. NUMERICAL SIMULATIONS

In numerical simulations we consider the perturbed SG model (3) where $F(x)$ is given by (4). Such a force creates a potential barrier at $x_* = 0$. The simulations are carried out using a lattice from -60 to 60 in the x direction. The values of the system parameters are chosen as $dt = 0.1$ for the time step, $\gamma = 0.01$ for the damping coefficient, and $t_{\max} = 60$ for the time of integration. The damping is introduced in the numerical simulations in order to reduce the numerical noise. The stability conditions are still valid. The initial conditions are

$$\phi(x, t=0) = 4\arctan(e^x), \tag{6}$$

$$\phi_t(x, t=0) = 0. \tag{7}$$

These conditions represent a stationary kink-soliton placed initially at the equilibrium position $x_* = 0$. To examine the accuracy of the simulation, we start with values of the control parameter B greater than one. Initially, the kink soliton translational mode is stable. The kink remains motionless at its equilibrium position. According to the stability analysis, for $1/3 < B^2 < 1$, the kink moves apart from $x_* = 0$. Indeed, a continuous displacement of the soliton is observed.

The first internal shape mode appears for $1/6 < B^2 < 1/3$. Despite the initial deformation, the stability of the shape mode prevents the breakup of the kink. For $B^2 < 5 + \sqrt{17}/2$ the kink soliton breaks up, and the formation of a kink-antikink

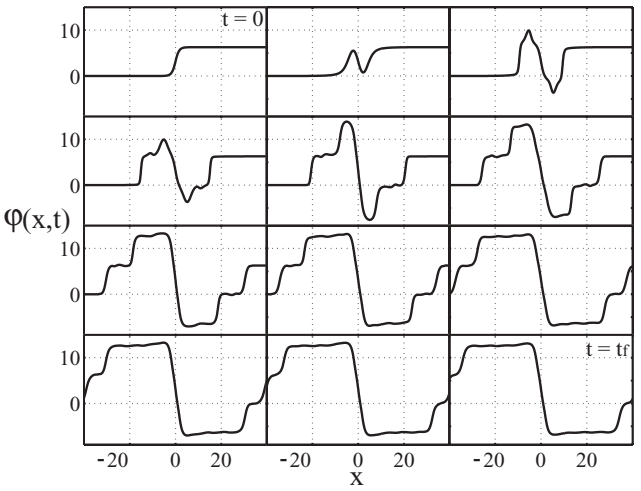

FIG. 1. Numerical simulation of (3) with $F(x)$ given by (4) under the threshold of shape instability ($B = 0.2564$). We can observe the formation of a two-kink soliton pair.

pair is observed. All the simulations exhibit a good agreement with the theory and the previous results (see Refs. [13,17,19]).

Beyond the shape instability threshold, an additional deforming structure is observed over each kink. Just below the threshold, this structure is not stable and disappears after some transient state. The final configuration is the expected kink-antikink-kink. Nevertheless, for $B = 0.2564$, the deforming structure is stable and generates a pair of two-kink solitons. Figure 1 shows the process described above. Both solitons are moving in opposite directions. Meanwhile, a motionless antikink soliton appears interpolating between -4π and 2π. If we continue decreasing the value of B, a multikink soliton pair is emitted and a large antikink (interpolating between 8π and -7π) is formed at $x_* = 0$ (see Fig. 2).

To obtain a clearer description of the mechanism involved in the formation of the two-kink pair, we perform a similar

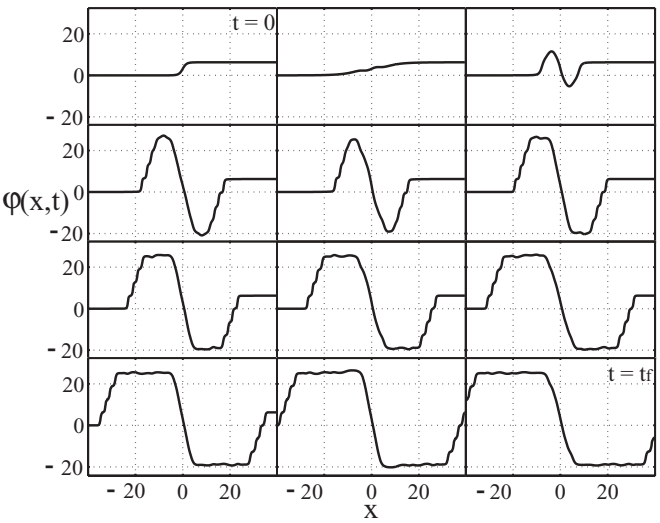

FIG. 2. Numerical simulations of (3) given by (4) for a lower value of B ($B = 0.2000$). A multikink soliton pair is emitted in opposite directions.

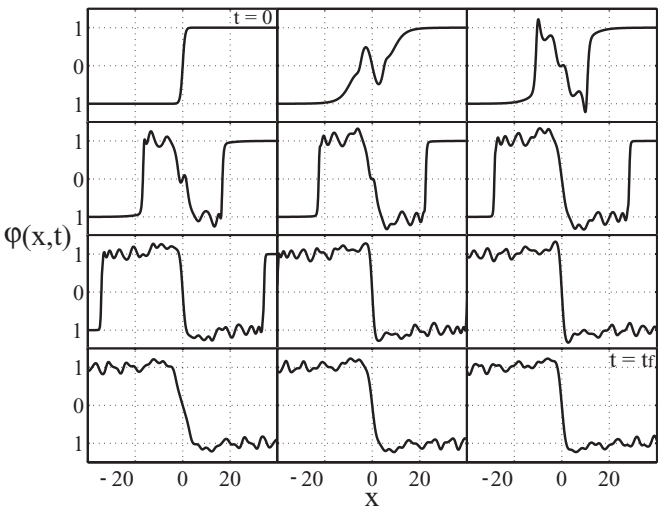

FIG. 3. Numerical simulations of (8) with $F(x)$ given by (9) and $B = 0.1100$. The formation of the two-kink soliton is not observed.

numerical study with the ϕ^4 model:

$$\phi_{tt} - \phi_{xx} - \tfrac{1}{2}\phi + \tfrac{1}{2}\phi^3 = F(x). \tag{8}$$

For this case $F(x)$ is given by

$$F(x) = \frac{1}{2}\frac{(4B^2 - 1)\sinh(Bx)}{\cosh^3(Bx)}. \tag{9}$$

Stability analysis establishes the instability threshold of the first internal shape mode at $B^2 < \frac{11-\sqrt{117}}{8}$. As expected, the breakup of a kink results from numerical simulations at this value. Below the shape instability threshold the formation of the two-kink soliton is not observed at any value of the control parameter B. Figure 3 displays the temporal evolution of a ϕ^4 kink perturbed by (9) for $B = 0.11$.

The simulations in both systems reveal that a multiple ground state degeneracy in the energy potential $U(\phi)$ is necessary for the existence of the two-kink soliton. According to the stability analysis, an internal shape mode instability leads to a kink-antikink pair creation. Notwithstanding, if the total energy is large enough, the multiple degeneracy of the ground state of $U(\phi)$ allows additional kink-antikink pairs to appear. A degeneracy similar to that appearing in the ϕ^4 model cannot form a two-kink soliton pair (Fig. 3) even if the amplitude of the external force is very large.

IV. ENERGY CONSIDERATIONS

As we have mentioned above, the appearance of the two-kink soliton is linked to the successive emission of kink-antikink pairs. Such an emission requires an extra amount of energy to be able to afford consecutive pairs formation. This energy is given by the external force and consequently a function of parameter B. Next, we show that the formation of a two-kink soliton can be predicted and controlled by varying external parameters.

The energy carried by a kink, in the unperturbed SG model, described by $\phi_0 = 4\arctan(e^{\pm\gamma(x-vt)})$ is $E = 8\gamma$ where v stands for the kink velocity and $\gamma = 1/(1 - v^2)$.

The perturbed nonlinear Klein-Gordon equation (1) can be derived from the following Lagrangian density:

$$\mathcal{L} = \tfrac{1}{2}\phi_t^2 - \tfrac{1}{2}\phi_x^2 - U(\phi) + F(x)\phi, \tag{10}$$

with the associated Hamiltonian density

$$\mathcal{H} = \tfrac{1}{2}\phi_t^2 + \tfrac{1}{2}\phi_x^2 + U(\phi) - F(x)\phi. \tag{11}$$

The energy conservation law can be written as $\frac{dH}{dt} = 0$, where $H = \int_{-\infty}^{\infty} \mathcal{H}\, dx$. If $\phi_k = 4\arctan(e^{Bx})$ and $U(\phi) = (1 - \cos\phi)$, then the total energy can be written as

$$H_T = H_k + H_{\text{ext}}, \tag{12}$$

where $H_k = \frac{4}{B}(B^2 + 1)$ represents the energy associated with the solution ϕ_k. H_{ext} is the extra energy given by the external force. Replacing $F(x)$ by expression (4), we obtain that

$$H_{\text{ext}} = -8(B^2 - 1)\int_{-\infty}^{\infty} \frac{\sinh(Bx)}{\cosh^2(Bx)} \arctan(e^{Bx})\, dx. \tag{13}$$

After an integration by parts, H_{ext} reads

$$\begin{aligned} H_{\text{ext}} &= -\frac{8(B^2-1)}{B}\left[\frac{2e^{Bx}\arctan(e^{Bx}) + 1}{e^{2Bx} + 1}\right]\Bigg|_{-\infty}^{\infty} \\ &= \frac{8(B^2-1)}{B}. \end{aligned} \tag{14}$$

Therefore, the expression for the total energy is

$$H_T = \frac{4}{B}(3 - B^2). \tag{15}$$

As we can see, the total energy increases with decreasing values of B. From the stability conditions, the first emission of a pair kink-antikink takes place when $B^2 < 1/6$. Using (15) with $B^2 = 1/6$, we are able to estimate the energy minimum value for the first kink-antikink pair creation: $H_T = 34\sqrt{6}/3 \approx 27.76$. By comparison with the energy related to ϕ_k, it is clear that the external force provides enough energy to produce an additional kink-antikink pair.

Using this criterion, we can get an estimate of the control parameter B at which the formation of the two-kink soliton pair takes place. The required energy to produce at least seven motionless solitons is $H_T = 56$. From (15), we obtain that the value of the control parameter that fulfills this condition is $B = 0.2111$ (the numerical simulations yield a close value, $B = 0.2465$). The reason for this difference can be understood by considering that the effective mass of propagative solitons differs from the motionless ones, resulting in a lower energy. In fact, numerical and experimental works report that the formation of bound states of kinks or multikink solitons can lead to a decrease of the associated energy due to a grow of their velocity [8–10]. Despite that, the energy criteria provide a very good estimation of the number of solitons produced after a kink internal mode instability.

V. FORMATION OF A PAIR OF TWO-KINK SOLITON

Formerly, we have discussed about the relevance of the emission of successive kink-antikink pairs in the two-kink formation. However, once two consecutive emissions of pairs are attained, the formation of a bound state between two kinks (antikinks) requires an additional ingredient.

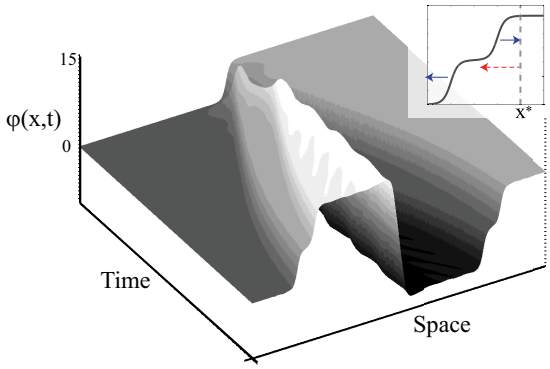

FIG. 4. (Color online) Space-time diagram of the two-kink soliton pair formation under the threshold of shape instability ($B = 0.2564$). Inset: Schematic plot that illustrates the direction of solitonic interaction forces (blue arrows) and the unstable (repeller) equilibrium position (dashed red arrow).

In a system with no external forces [$F(x) = 0$], two single solitons interact with each other through a repulsive force which decays with the distance between their mass centers [21]. Such an interaction will separate them, preventing a binding process. On the other hand, the zeros of the external force [e.g., Eq. (4)] are equilibrium positions. When these positions are unstable, the kink solitons move away from them. This cause an opposite effect to the repulsive force. Making possible the formation of a two-kink soliton (see Fig. 4). Inset in Fig. 4 shows a schematic representation of this interplay. Two kink solitons are located on the right (or on the left) of the unstable equilibrium point located at $x^* = 0$. Both kinks move away from this equilibrium point (red arrow) preventing the separation (blue arrows).

To understand this phenomenon, we introduce a new state which represents two standard kinks separated by a distance d and parametrized by B:

$$\phi_{k_0} = 4\arctan(e^{B(x+d)}) + 4\arctan(e^{B(x-d)}). \tag{16}$$

Following an inverse problem method,

$$F_0(x) = \sin[\phi_{k_0}] - \phi_{k_0 xx}, \tag{17}$$

we are able to build a suitable model which supports the two-kink soliton solution under the presence of an external forcing. The calculated external force F_0 is

$$\begin{aligned} F_0(x) = {} & 2(B^2 - 1)[\alpha_+\beta_+ + \alpha_-\beta_-] \\ & + 4[\alpha_+\beta_+\alpha_-^2 + \alpha_-\beta_-\alpha_+^2], \end{aligned} \tag{18}$$

where $\alpha_\pm = \operatorname{sech}[B(x \pm d)]$ and $\beta_\pm = \tanh[B(x \pm d)]$.

It is easy to observe that the above function represents an external force parametrized by B with three equilibrium positions located at $x_* = 0$ and $x_* = \pm d$. In Fig. 5 we illustrate the force F_0 for different values of d. The equilibrium position (zero of function F_0) located at $x_* = 0$ represents a stable (unstable) point for a kink (antikink) (blue filled dot) while $x_* = \pm d$ act on a kink (antikink) as unstable (stable) points (red circles).

For $d = 0$ the separation between different equilibrium positions is a minimum and $\frac{\partial F(x)}{\partial x}|_{x^*=0}$ is a maximum. The effective potential created by F_0 at $x = 0$ restrains the repulsive

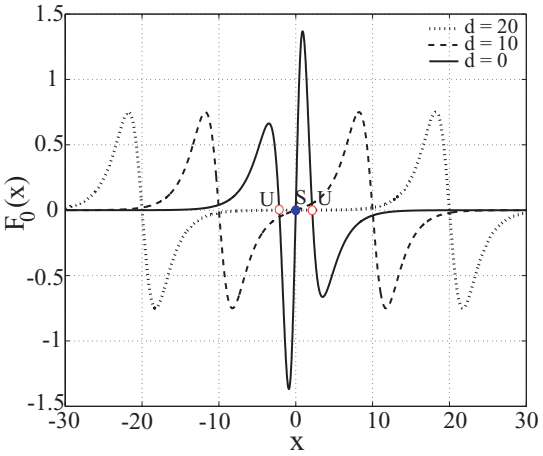

FIG. 5. (Color online) Function $F_0(x)$ given by Eq. (18) at $B = 0.5000$ for different values of d. The zeros of the force act as stable (Filled blue dots) or unstable (Open red circles) equilibrium positions.

interaction force between the two kinks. Thus, for values of B below the shape instability threshold the initial state remains located at $x_* = 0$ without any deformation. In Fig. 6 we can observe this behavior.

For values of $d \neq 0$, $\frac{\partial F(x)}{\partial x}|_{x^*=0}$ diminishes as d increases. An initial separation of the two original kinks is observed. This effect is displayed in Fig. 7. However, $x_* = \pm d$ act as repelling points. Thus, the two kinks will separate from each other until they reach an equilibrium between both unstable positions (see Fig. 7). The numerical simulation also reveals that the kink asymptotic zones (wings) undergo a shape instability close to x_*. However, the energy is not enough (above the critical threshold) to produce an additional kink-antikink pair.

Next, we discuss the dynamics when the shape mode is unstable and $d \neq 0$. At a first stage, the initial two kinks repel each other, moving towards the points $x_* = \pm d$. Notwithstanding, the shape instability is strong enough to produce a kink breakup creating two kinks, moving in opposite

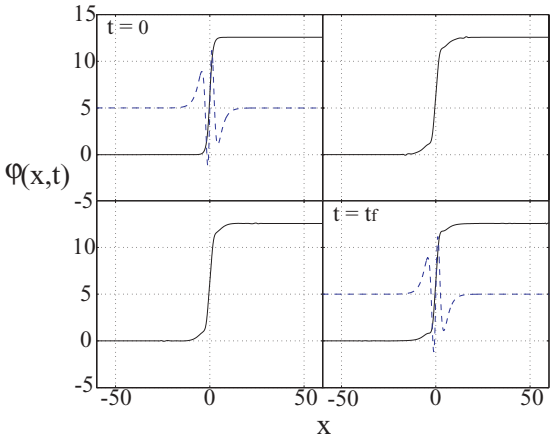

FIG. 6. (Color online) Numerical simulation of (3) with $F_0(x)$ given by (18), $d = 0$, $B = 0.5000$, $dt = 0.1$, $\gamma = 0.01$, and $t_{\max} = 60$. The original state composed of two kinks remains located at $x = 0$ without any deformation. Dotted blue line: External force $F_0(x)$ illustrated in order to show equilibrium positions (not scaled).

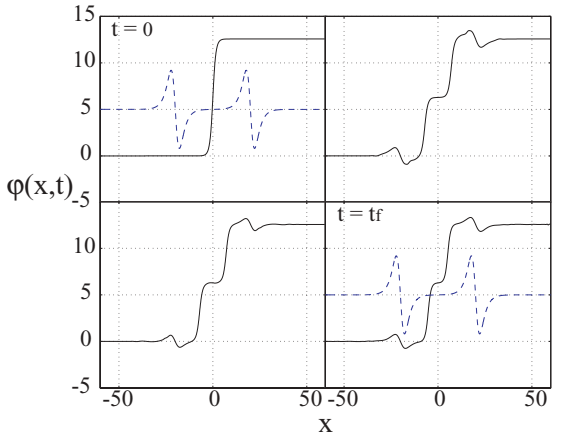

FIG. 7. (Color online) Numerical simulation of (3) with $F_0(x)$ given by (18), $d = 20$, $B = 0.5000$, $dt = 0.1$, $\gamma = 0.01$, and $t_{\max} = 60$. The original state composed of two kinks separates, reaching an equilibrium between both unstable positions located at $x = \pm d$. Dotted blue line: External force $F_0(x)$ illustrated in order to show equilibrium positions (not scaled).

directions and a two-antikink soliton in both sides of $x^* = 0$. The kink created on the left (right) of the point $x = d$ ($x = -d$) is attracted by the position $x = 0$ (stable position for a kink), giving rise to a packed state (a multikink soliton) located at $x = 0$. The same behavior is observed for the two-antikink formed at $x = \pm d$ (stable position for antikinks), where we can see a "packed" state of two antikinks. Meanwhile, the two kinks formed on the right (left) of the point $x = d$ ($x = -d$) are repelled by this point and they move away from it. Figure 8 shows the whole dynamics described above. The dynamics described above also explain the apparent nonexistence of a multi-antikink in our original perturbed SG model. For an antinkink, the point $x^* = 0$ is a stable equilibrium. The point $x = 0$ represents a stable equilibrium position for antikinks.

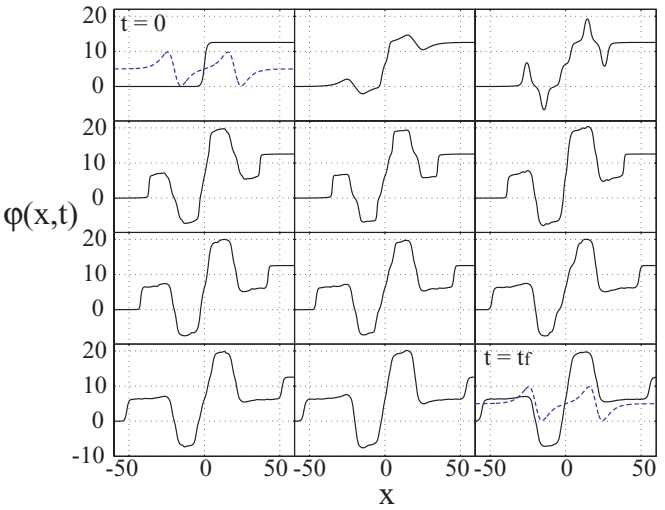

FIG. 8. (Color online) Numerical simulation of (3) with $F_0(x)$ given by (18), $d = 20$, $B = 0.2000$, $dt = 0.1$, $\gamma = 0.01$, and $t_{\max} = 60$. Separation, breakup, and packing processes of solitons in sequence. Dotted blue line: External force $F_0(x)$ illustrated in order to show equilibrium positions (not scaled).

The attraction by $x = 0$ compresses them together such that there is no distance of separation between different antikinks, forming a packed state. Figures 1 and 2 exhibit the formation of packed states of three-antikink and seven-antikink solitons, respectively.

Note that despite the special construction of (18) using the geometrical theory of dynamical systems, all the results can be extended to any model topologically equivalent to those shown here. Therefore, similar systems which possess the same topological characteristics of the force could display a two-kink soliton formation.

VI. TWO-KINK SOLITONS IN JOSEPHSON JUNCTIONS

The initial formulation of a family of scalar models where the two-kink soliton appears as a solution was motivated for its implications on the field of the string theory, particularly, in the brane world. In this context, the soliton structure (considered as a defect or a domain wall) can be used to mimic a thick brane (membrane) on a hyperdimensional volume [5–7].

Recent works, however, have shed light on new experimental perspectives in which the two-kink soliton can be studied. In Ref. [22] the authors showed that a domain wall profile in a magnetic material can be manipulated by geometrical constraints so that a two-kink soliton can be formed.

In this regard, an interesting experimental device in soliton dynamics is the long Josephson junction (LJJ) and its discrete version, the Josephson array. A regular kink in a LJJ corresponds to a Josephson vortex or fluxon, a quantum of magnetic flux. The fusion of two regular fluxons (kinks) into a bound state (two-kink soliton state) has already been reported in an annular Josephson array subject to a constant bias current [8–10]. These works refer to the surface losses as the responsible for soliton bunching in LJJs.

Moreover, additional works [23,24] have described a method to create Fluxon-antifluxon (kink-antikink) states using a "current dipole." The technique consists in injecting into the junction a relatively large current that is collected back at another point of the same electrode, which is separated from the injection spot by a small distance D. A remarkable feature of this setup is that the injected-current profile displays a spatially dependance similar to the external force (4). The amplitude of the external force is proportional to the current I analogously to our control parameter B. Based on this, we propose a possible experiment in order to observe the formation of a two-kink soliton due to an internal mode instability in a real physical system such as a Josephson junction. The experimental setup, consisting of a LJJ driven by a current dipole and a bias current, reproduces the forcing conditions of our numerical simulations. The motion of the soliton can be measured by analyzing the current-voltage characteristics. The soliton velocity is proportional to the voltage V. It has been reported that the velocity of a two-kink state is significantly higher than the velocity of a single kink, rendering the formation of bound states as the two-kink soliton easy to detect [8–10]. Thus, Joshepson junctions represent a very practical way to explore the formation of multikink states. This has interesting implications in the field of high-energy particles and cosmology, where the formation of particles in the presence of external fields represents an active research field.

VII. CONCLUSIONS

We show the formation of a two-kink soliton pair in the perturbed sine-Gordon model due to internal mode instabilities. The conditions for the formation of this kind of solutions are a combination of instabilities in the shape internal modes and an effective potential created by an external force. These results show that the external force plays an important role in the formation process of other types of solutions as multikinks via the separation or the "packing" of several kinks (antikinks). A possible experimental setup with interesting implications in the field of high-energy particles and cosmology is proposed.

ACKNOWLEDGMENTS

The authors thank J. Toro-Mendoza for fruitful discussions. M.A.G.-N. thanks FONDECYT project 3110024 for partial funding support.

[1] T. Dauxois and M. Peyrard, in *Physics of Solitons*, edited by N. York (Cambridge University Press, Cambridge, 2006).
[2] J. A. González and J. A. Holyst, Phys. Rev. **35**, 3643 (1987).
[3] D. Bazeia, J. Menezes, and R. Menezes, Phys. Rev. Lett. **91**, 241601 (2003).
[4] D. Bazeia, L. Losano, J. Malbouisson, and R. Menezes, Physica D **237**, 937 (2008).
[5] A. de Souza Dutra, Physica D **238**, 798 (2009).
[6] A. E. R. Chumbes and M. B. Hott, Phys. Rev. D **81**, 045008 (2010).
[7] D. Bazeia, J. Furtado, and A. R. Gomes, JCAP 02 (2004) 002.
[8] A. V. Ustinov, B. A. Malomed, and S. Sakai, Phys. Rev. B **57**, 11691 (1998).
[9] J. Pfeiffer, M. Schuster, A. A. Abdumalikov Jr., and A. V. Ustinov, Phys. Rev. Lett. **96**, 34103 (2006).
[10] B. A. Malomed, Phys. Rev. B **47**, 1111 (1993).
[11] A. R. Champneys and Y. S. Kivshar, Phys. Rev. E **61**, 2551 (2000).
[12] A. A. Aigner, A. R. Champneys, and V. M. Rothos, Physica D **186**, 148 (2003).
[13] J. A. González and J. A. Holyst, Phys. Rev. B **45**, 10338 (1992).
[14] Y. S. Kivshar and B. A. Malomed, Rev. Mod. Phys. **61**, 763 (1989).
[15] A. Barone and G. Paternó, in *Physics and Applications of the Josephson Effect*, edited by N. York (Interscience, New York, 1982).
[16] C. B. Tabi, A. Mohamodau, and T. C. Kofané, Phys. Scr. **77**, 045002 (2008).
[17] J. A. González, A. Bellorín, and L. E. Guerrero, Phys. Rev. E **65**, 065601 (2002).

[18] J. A. González, A. Bellorín, and L. E. Guerrero, Phys. Rev. E **60**, 37R (1999).

[19] J. A. González, M. A. García-Nustes, A. Sánchez, and P. V. E. McClintock, New J. Phys. **10**, 113015 (2008).

[20] J. A. González, S. Cuenda, and A. Sánchez, Phys. Rev. E **75**, 036611 (2007).

[21] B. A. Mello, J. A. González, L. E. Guerrero, and E. Lopez-Atencio, Phys. Lett. A **244**, 277 (1998).

[22] P. O. Jubert, R. Allenspach, and A. Bischof, Phys. Rev. B **69**, 220410(R) (2004).

[23] B. A. Malomed and A. V. Ustinov, Phys. Rev. B **69**, 064502 (2004).

[24] A. V. Ustinov, Appl. Phys. Lett. **80**, 3153 (2002).